Stirling 1984

THEORETICAL AND EXPERIMENTAL STUDY OF THE INLET AND OUTLET CAVITATION IN A MODEL OF A FRANCIS TURBINE

by

F AVELLAN AND P HENRY

SWISS FEDERAL INSTITUTE OF TECHNOLOGY

PAPER 1.3

THE 12TH IAHR SYMPOSIUM, STIRLING

27-30 AUGUST 1984

THEORETICAL AND EXPERIMENTAL STUDY OF THE INLET AND OUTLET CAVITATION IN A MODEL OF A FRANCIS TURBINE

F. Avellan, Research Scientist and
P. Henry, Professor
Hydraulic Machines and Fluid Mechanics Institute, Swiss Federal Institute of Technology, Lausanne

SYNOPSIS

In order to study the inlet and outlet cavitation in a Francis turbine ($n_q = 48$) a numerical model of the bubble dynamics is established. By using the pressure and velocity distribution obtained by a 3-D potential flow analysis of the turbine, the Rayleigh-Plesset equation is integrated for a wide range of head and bubble sizes and for two typical turbine operating points, where inlet and outlet cavitation respectively are observed.

The numerical simulations agree very well with the main cavitation features observed in the turbine runner.

The minimum explosive bubble radius is found to be an inverse function of the test head, as predicted by the equilibrium free nucleus stability theory, unless this theory overestimates the size of the minimum active nuclei, mainly in outlet cavitation.

Hence, these results, in addition to a measured water nuclei radii histogram, can explain fairly well both the influence of water nuclei content in outlet cavitation and the inlet cavitation independence of this content for usual test heads.

The test head is then found to influence the maximum explosive bubble sizes by an $H^{-\frac{1}{2}}$ law.

THEORETICAL AND EXPERIMENTAL STUDY OF THE INLET AND OUTLET CAVITATION IN A MODEL OF A FRANCIS TURBINE

F. Avellan and P. Henry

1. INTRODUCTION

The effect of the head on the performance of a cavitating Francis turbine is known in hydraulic turbomachinery model testing. This effect has been studied by many authors, including Henry and Lecoffre [1] . The influence of water nuclei content has been shown in the travelling cavitation (separate bubble flow) occurring at the blade outlet of a Francis turbine.

The first aim of this study is to extend the qualitative results of reference [1] by using the Rayleigh-Plesset equation and by performing experiments on a Francis turbine model ($n_q = 48$).

The second aim is to study the influence of the head and the water nuclei content on Francis turbine inlet edge cavitation, which was not studied in the work mentioned above. This cavitation feature is examined in the same way as the outlet cavitation case by using numerical simulation and experiments.

The experiments on the Francis turbine model were carried out in the laboratory of the Hydraulic Machines and Fluid Mechanics Institute.

The numerical simulations of the different cavitation cases were obtained by feeding three-dimensional flow analysis data into the driving terms of the Rayleigh-Plesset equation.

2. RAYLEIGH-PLESSET MODEL OF FRANCIS TURBINE CAVITATION REGIME

It is possible to describe the Francis turbine cavitating flow, as shown in Figures 8 and 9, by transient cavity dynamics. By assuming that the cavity dimensions remain small compared with the macroscopic flow scale, the Rayleigh-Plesset equation [2] can be applied with the following assumptions.

a) Cavities are spherical and their radii are small enough to be neglected in a first order analysis. So, the bubbles do not disturb the macroscopic flow.

b) Spherical cavities follow the macroscopic stream lines.

c) The flow of the microscopic field surrounding the cavity is incompressible and potential.

d) The cavity is initially in an equilibrium state and during its evolution no mass or heat transfer occurs.

e) The non-condensable gas inside the cavity expands, following an adiabatic law.

These assumptions allow us to write the Rayleigh-Plesset equation in the following form:

$$R\ddot{R} + \frac{3}{2}\dot{R}^2 + \frac{4\nu}{R}\dot{R} = \frac{1}{\rho}\left[P_V - P(t) - \frac{2\gamma}{R} + \left[\frac{2\gamma}{R_o} - (P_V - P_o)\right]\left(\frac{R_o}{R}\right)^{3\Gamma}\right] \quad (1)$$

where:

R	: bubble radius of initial value R_o	(m)
P_V	: vapour pressure	(Pa)
$P(t)$	: bubble far field pressure, given by the flow, of initial value P_o	(Pa)
γ	: gas-liquid surface tension	(N/m)
ν	: liquid cinematic viscosity	(m^2/s)
ρ	: liquid density	(kg/m^3)
Γ	: ratio of the specific heats of the gas	(-)

The dots denote differentiation with respect to time t.

To normalise the Rayleigh-Plesset equation it is useful to choose the turbine parameters characteristic of the flow. For a given operating point and a given turbine blade profile of chord L, the choice of the head will give the bubble passing time over the blade profile and the relative pressure $(P(t) - P_{ref})$ as a function of time. Furthermore, a reference pressure P_{ref} should be chosen, usually the turbine cavitation coefficient σ is introduced, which gives an absolute total pressure level, upstream or downstream of the runner.

Consequently, the upstream absolute pressure P_o of equation (1) will be different for each streamline profile. For this reason it is more convenient to define a cavitation number σ_p, relative to each streamline profile, by the following expression

$$\sigma_p = \frac{P_o - P_v}{\rho g H}$$

where g is the gravity acceleration.

With the chord L and the head H as normalisation parameters, equation (1) becomes:

$$\ddot{r}\,r + \frac{3}{2}\dot{r}^2 + \frac{4}{Re}\frac{\dot{r}}{r} = -\frac{\sigma_p + C_p(t')}{2} - \frac{2}{W_e^2}\frac{1}{r} + \frac{G}{2}\frac{1}{r^{3\Gamma}} \quad (2)$$

where:

$r = \frac{R}{L}$ normalised radius (-)

$$C_p(t) = \frac{P(t) - P_o}{\rho g H}$$ pressure coefficient (-)

$$W_e^2 = \frac{2\rho g H L}{\gamma}$$ Weber number (-)

$$Re = \frac{\sqrt{2gH}\, L}{\nu}$$ Reynolds number (-)

$$G = (\sigma_p + \frac{4}{W_e^2}\frac{1}{r_o})r_o^3\Gamma$$ gas content number (-)

The dots denote differentiation with respect to normalised time t' given by

$$t' = \frac{L}{\sqrt{2gH}}\, t$$

Form (2) of the Rayleigh-Plesset equation can be compared with the normalised form given by Arndt [3] , where the upstream velocity is related to the turbine head.

For a given pressure distribution C_p and with the basic assumption that bubbles start to grow from an equilibrium state, equation (2) depends on three parameters: σ_p , Weber number We and Reynolds number Re. Theoretically, to perform similar tests using a model turbine, these three parameters should be held constant in such a way that, if the initial bubble radius scales with the turbine size, the resulting bubble dimension should also scale with the turbine size. The relation between the Weber number and the Reynolds number prevents us from using the similarity principle between model and prototype.

3. SOLUTION OF THE RAYLEIGH-PLESSET EQUATION IN A FRANCIS TURBINE AND COMPARISON WITH EXPERIMENTS

The Rayleigh-Plesset equation is solved numerically by a Runge-Kutta integration technique for a Francis runner designed by the Hydraulic Machines Institute $n_q = 48$, see Figures 1 and 2. The flow calculation was made with an improved 3-D finite element potential flow program, property of Dominion Engineering Works Ltd [4] .

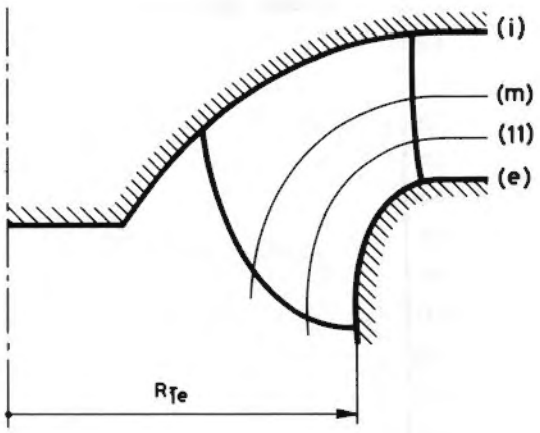

Figure 1: Meridional view of the runner

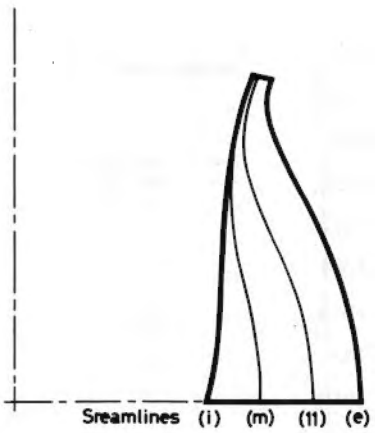

Figure 2: The suction side, seen from above

The pressure and velocity field is available on a three-dimensional runner channel mesh, for two operating points corresponding to the best efficiency point and to a slightly higher head point respectively. These two points are represented on the hill chart in Figure 3.

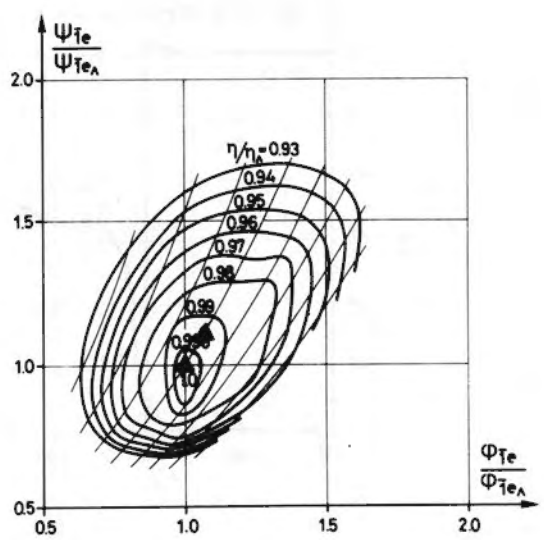

Figure 3: Non-dimensional turbine hill chart

The pressure distributions of interest were normalised with the proper turbine model data and plotted in Figures 4 and 5. The velocity field is integrated along a bubble trajectory with respect to time to obtain the function $C_p(t')$. The results for the two operating points are given in Figures 6 and 7. For a more explicit representation the C_p distribution is given as a function of x/L.

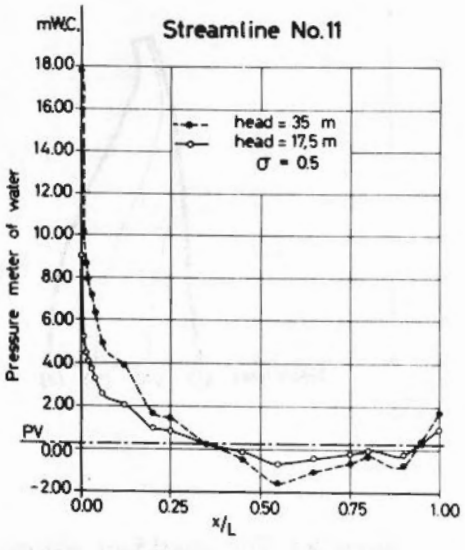

Figure 4: Absolute pressure distribution for the best efficiency point

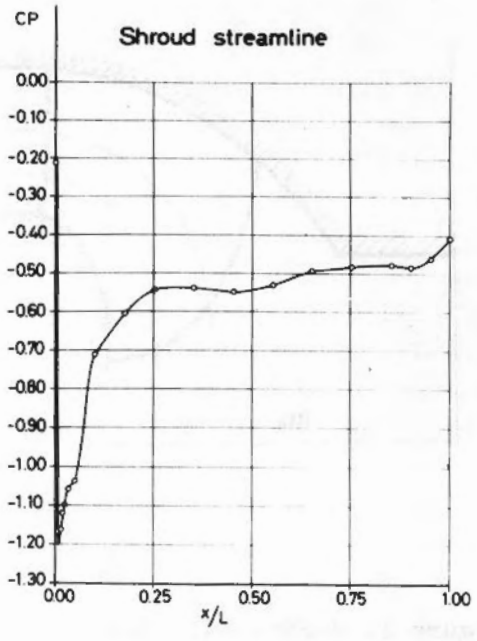

Figure 5: C_p distribution for the high head point

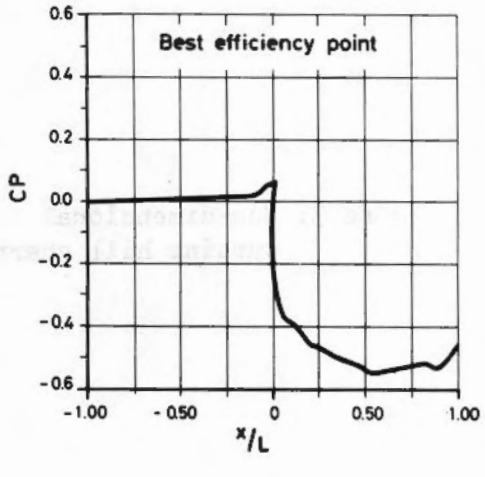

Figure 6: Bubble pressure coefficient as function of x/L along the streamline 11 at the best efficiency point

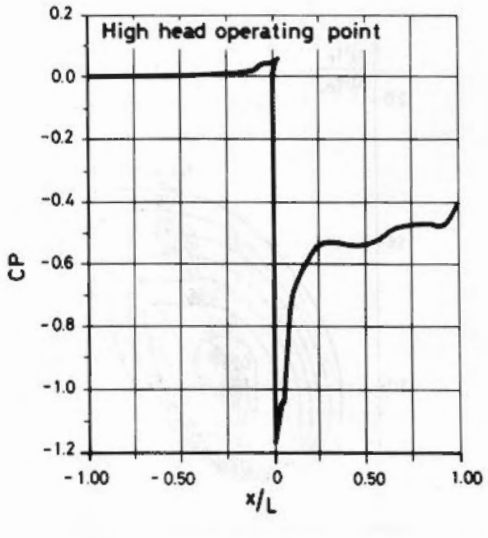

Figure 7: Bubble pressure coefficient as function of x/L along the shroud streamline at the high head point

If a bubble is followed from the upstream coordinate (x/L = -1) the bubble is slightly compressed until it reaches the stagnation point region. It is then exposed to a low pressure on the blade suction side (Figures 6 and 7).

The main difference between the two operating points is the sharp under-pressure peak corresponding to the flow incidence increase at the high head point (Figures 6 and 7).

To check the Rayleigh-Plesset equation solution, a model turbine test is performed with the same conditions as the Rayleigh-Plesset equation solution, i.e. with the same operating points, the same heads and the same corresponding turbine cavitation coefficients. Photographs of these tests are shown in Figures 8 and 9.

Figure 8: Photograph of outlet cavitation at the best efficiency point,
H = 35 m
σ = 0.052

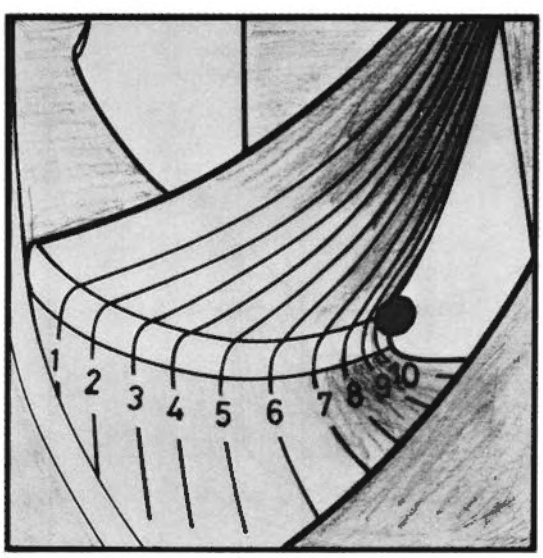

Figure 9: Photograph of inlet cavitation at the high head point
H = 30 m
σ = 0.08

The two operating points correspond to different kinds of cavitation: inlet and outlet. At the inlet cavitation operating point a higher cavitation number is chosen to avoid the outlet cavitation.

In the outlet cavitation case, corresponding to the best efficiency point, see Figure 8, bubbles start to grow for $x/L \sim 0.45$ and the maximum bubble size can be evaluated at a diameter of about 2 mm. These measurements were done by using reference marks on the blade suction side shown in Figure 10.

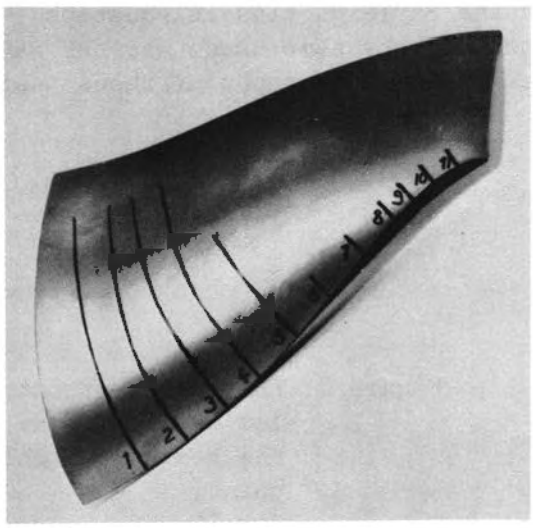

Figure 10: Photograph of the original blade suction side with reference marks

By solving the Rayleigh-Plesset equation for the same conditions, H = 35 m, σ_p= 0.5 and for 1.5 - 100µm initial radii range we obtain the radii evolution over the blade, Figure 11.

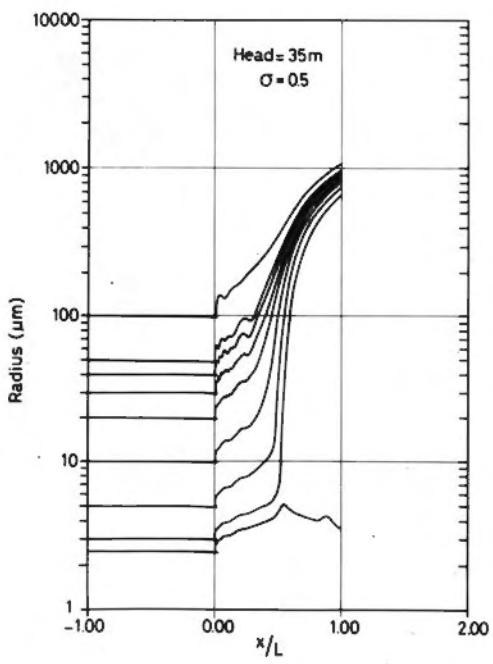

Figure 11: Rayleigh-Plesset solutions for the best efficiency point,
H = 35 m
σ_p = 0.5

Bubbles are subjected to a slight radius decrease until they reach the stagnation point region and then they grow. Two drastically different behaviours can be seen depending on the initial size of the bubbles.

For the smallest initial radius, 5 μm, the bubble simply follows the pressure distribution to which it is subjected.

Meanwhile, for larger bubble radii the bubble growth takes place in the same way as for the smallest radius until it reaches the point $x/L \sim 0.41$ where explosive growths occur. Even with a pressure increase from $x/L \cong 0.5$, see Figure 5, the bubbles continue to grow beyond the trailing edge. For explosive bubbles a radius range of 2-100 μm at $X/L = -1$ can be observed. This is reduced to a range of 700-1000 μm at $X/L = 1$. The maximum radii obtained at the trailing edge agree with the 2 mm diameters estimated from the photograph (Figure 8).

In the inlet cavitation case, corresponding to the high head operating point, see Figure 9, bubble collapse occurs for $x/L \sim 0.1$. Unfortunately the bubbles were too small to allow an estimate of their diameters by a simple observation through the transparent model draught tube cone. However, the cavitation looks like a small bubble cluster instead of a single cavity.

For the same condition, $H = 30$ m, $\sigma_p = 0.8$, Rayleigh-Plesset equation solutions for a 1-50 μm initial radii range are plotted in Figure 12. A similar growth behaviour to that of the outlet case is observed, unless the bubbles start to explode at the leading edge $x/L = 0$.

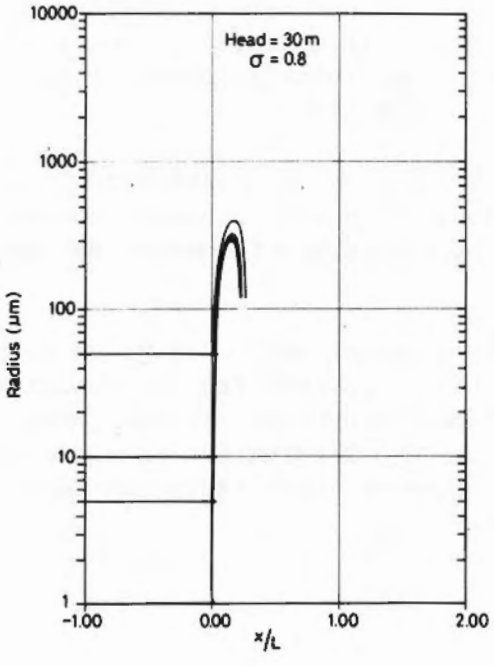

Figure 12: Rayleigh-Plesset solutions for the high head point
$H = 30$ m
$\sigma_p = 0.8$

Over the blade the bubbles reach a maximum radius at $x/L \sim 0.16$ and then collapse occurs at $x/L \sim 0.25$.

As in the outlet cavitation case, there is a radius below which no explosion occurs.

The difference according to calculated and observed collapse location can be explained by the low theoretical minimum value of C_p, see Figure 7.

The current practice in model cavitation testing is to choose an arbitrary head because of the lack of knowledge about the similarity laws.

Because of this difficulty the nuclei content and the head effect influence are examined below, with the help of experiments and calculations based on the Rayleigh-Plesset model.

Notwithstanding the crude approximations leading to these numerical results, the Rayleigh-Plesset model still gives good qualitative results and it predicts the outlet cavitation case accurately.

4. STUDY OF WATER NUCLEI CONTENT INFLUENCE AND HEAD EFFECT ON OUTLET CAVITATION

4.1 Water Nuclei Content Influence

In the past few years the water nuclei content influence on cavitation behaviour has been studied. The influence of nuclei injection on the efficiency curve plotted as a function of σ_p was shown in [1] .

This problem has received attention in the literature, see for instance the extensive study with valve experiments made by Oldenziel [5] .

The nuclei population influence can be illustrated by comparing Figures 13 and 14. The only difference between these photographs is a nuclei injection during the test corresponding to Figure 14.

The water nuclei content can be defined by two parameters: the minimum active nuclei radius of the population and the active nuclei concentration. A nucleus is said to be active if an explosive growth occurs during its passage over the blade.

By assuming that the minimum active nuclei radius is given by the minimum critical free nuclei radius, Henry and Lecoffre [1] explained the influence of nuclei injection on performance curves. Thereby, the critical pressure concept is established from the equilibrium free nucleus stability theory [6] . In order to see the validity of this theory the Rayleigh-Plesset model developed above is used.

Figure 13: Photograph of outlet cavitation at the best efficiency point
H = 17.5 m
σ = 0.052

Figure 14: Photograph of outlet cavitation with the same operating condition as Figure 13 with a nuclei injection

To find the lowest radius limit for which an explosive growth occurs the Rayleigh-Plesset equation is solved at the same σ_p, for different heads, by varying the initial radius.

The results obtained are plotted in Figure 15 both on linear and logarithmic scales and compared with the critical pressure theory. Owing to dynamic effects, bubbles with radii smaller than the critical radii explode. The curve corresponding to the Rayleigh-Plesset model has the same relation to the head, H^{-1}, as the curve obtained by the critical pressure theory. However, for the same head the bubble radius obtained with the Rayleigh-Plesset model is 2.4 times smaller than the one obtained with the critical pressure theory.

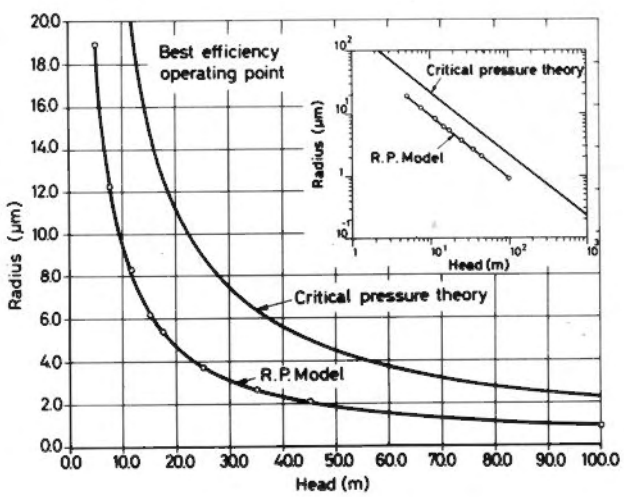

Figure 15: Minimum active nuclei radius versus head obtained by the critial pressure and by Rayleigh-Plesset theories at the best efficiency point, σ_p = 0.5

In other words, during a model test at a given σ_p, the lowest nuclei radii limit and the nuclei concentration of the water nuclei content will be fixed by the resorption characteristic of the test loop, by the water-air content and by the test head. For instance, by assuming a lowest radii limit of 5 μm, the critical pressure theory suggests a test head of 45 m in order to activate all the nuclei. The more realistic Rayleigh-Plesset model gives a 19 m test head.

In order to check the nuclei size distribution in the water, a measurement was made with a venturi system [7] . The results obtained are plotted in Figure 16 in terms of a radius histogram. The dissolved oxygen content during the test is 2.5 p.p.m. The surprisingly small nuclei sizes can be explained by the long degassing time which preceded the model test.

These sizes are typical and most cavitation tests are performed under these conditions in many laboratories.

Hence, the usual practice of degassing the water for cavitation testing reduces the water nuclei sizes and increases the influence of the test head on the active nuclei content.

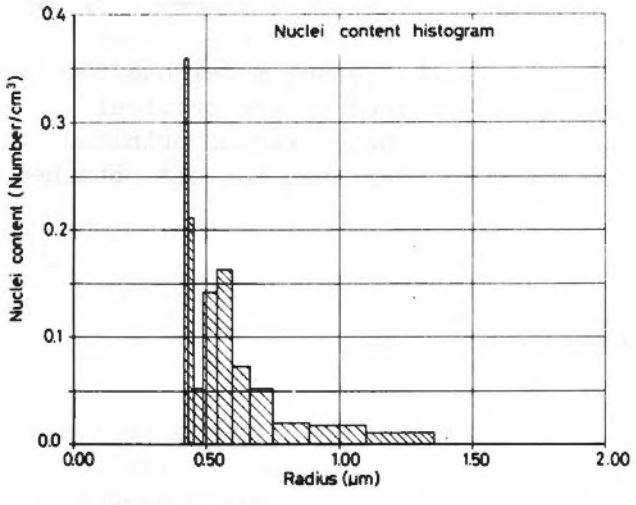

Figure 16: Radius histogram for degassed water: dissolved oxygen content = 2.5 p.p.m.

4.2 Head Effect

In order to investigate the head effect, two different tests were performed with the same cavitation number, for two different heads, 17.5 m (see Figure 13) and 35 m (see Figure 8) respectively. A careful observation of these photographs shows the smallest bubble sizes in the highest head case. Unfortunately, the model construction limitation prevents us increasing the head, hence preventing the observation of significant size differences.

Nevertheless the Rayleigh-Plesset equation solutions for a wide range of heads, 17.5 m, 35 m and 100 m (Figures 17, 12 and 18 respectively) show this decreasing trend of maximum radii with a head increase.

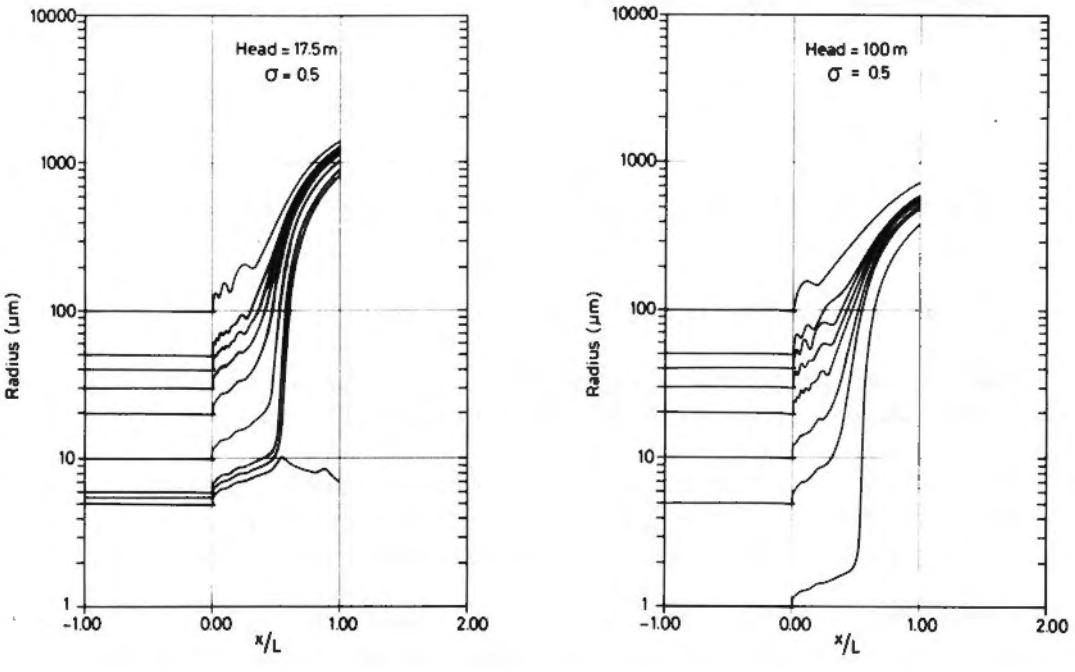

Figures 17 and 18: Rayleigh-Plesset solutions for the best efficiency point, H = 17.5 m, 100 m respectively, $\sigma_p = 0.5$

This trend is more significantly illustrated in Figure 19 where the maximum radius, reached for x/L = 1 and corresponding to the smallest active bubble radius, is plotted for each head. The curve plotted in Figure 19 is obtained by a least squares fit of the data according to an $H^{-\frac{1}{2}}$ law.

The agreement of this law with the Rayleigh-Plesset model results, in spite of the scatter generated by the lack of calculation accuracy, suggests that the explosive bubble size should be scaled by an $H^{-\frac{1}{2}}$ law.

Hence for higher heads bubbles have less time to grow than for lower heads.

Therefore, by comparing the H^{-1} scaling law of the smallest active nuclei radius and the $H^{-\frac{1}{2}}$ scaling law of the explosive nuclei radius, the head effect on bubble size would be of second order importance relative to the water nuclei content influence.

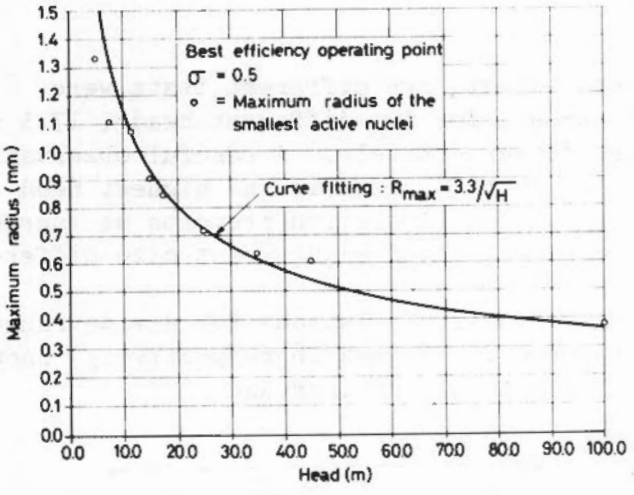

Figure 19: Maximum radius of the smallest active nuclei versus head, best efficiency point, $\sigma_p = 0.5$

5. STUDY OF WATER NUCLEI CONTENT INFLUENCE AND HEAD EFFECT ON INLET CAVITATION

5.1 Water Nuclei Content Influence

By comparing the photographs in Figure 21 no difference can be seen in the inlet cavitation appearance in spite of a nuclei injection.

The inlet cavitation independence of the water nuclei content may be explained with the help of Figure 20. The curves plotted in this figure are obtained in a similar way to the curves plotted in Figure 15.

The two curves are close together and they obey the same H^{-1} relation. It can be seen that in practice all the nuclei are activated even for such a small head as 10 m. Hence, by varying the head between 15 m (Figure 23) and 30 m (Figure 12), no more nuclei will be activated.

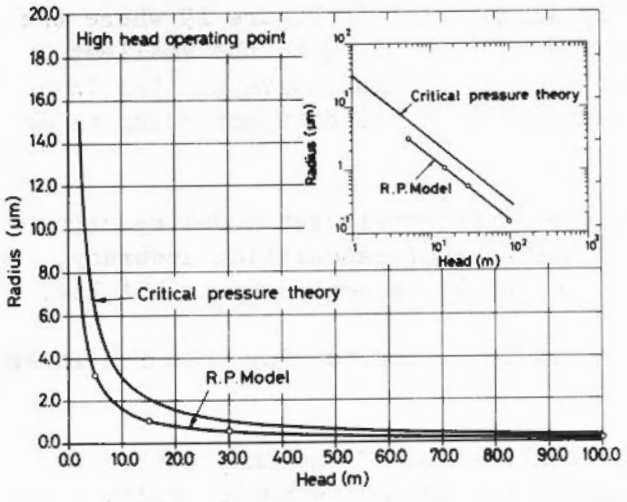

Figure 20: Minimum active nuclei radius versus head obtained both by the critical pressure theory and by the Rayleigh-Plesset solutions at the high head point, $\sigma_p = 0.8$

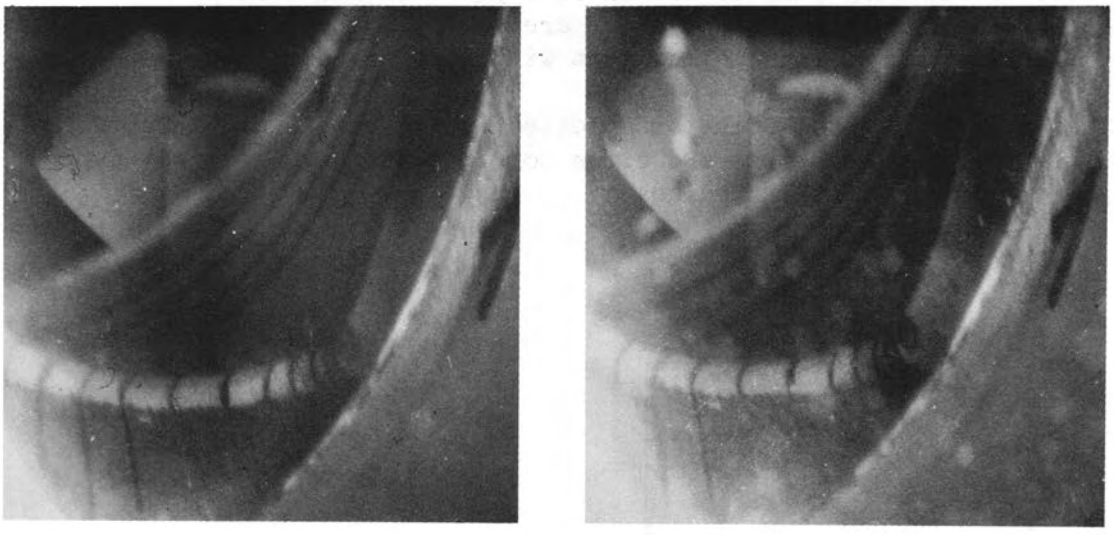

Figure 21: Photographs of inlet cavitation at the high head point
H = 15 m, σ = 0.08

Photo on the left: without nuclei injection
Photo on the right: with nuclei injection

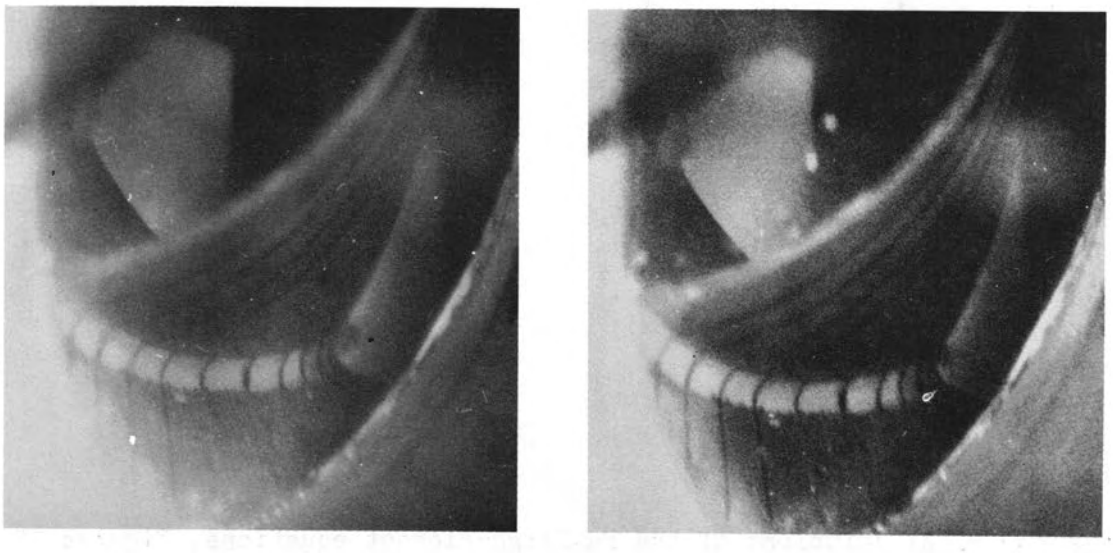

Figure 22: Photographs of inlet cavitation at the high head point,
H = 30 m, σ = 0.08
Photo on the left: without nuclei injection
Photo on the right: with nuclei injection

Further, the 3-D flow calculation shows a small low-pressure area which corresponds very well to the cluster position and size of the small bubbles observed in the machine. This area seems to be saturated by bubbles and an increase of water nuclei content will not increase the cluster size.

The Rayleigh-Plesset solutions plotted in Figures 12 and 13 show that the bubble collapse locations are close together and have a slight dependence on the initial bubble radius.

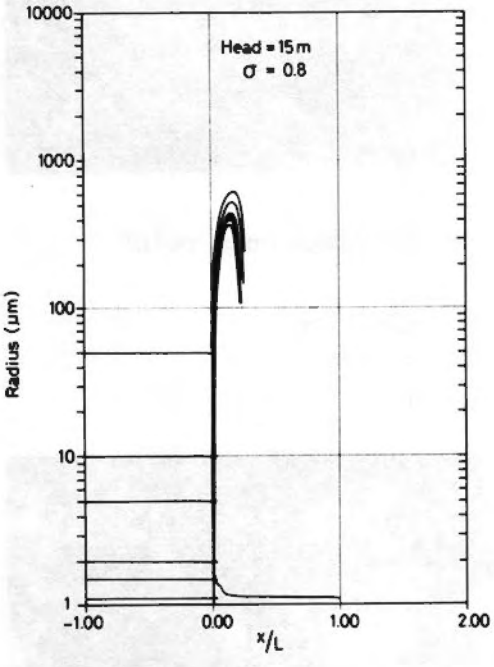

Figure 23: Rayleigh-Plesset solutions for the high head point
H = 15 m
σ_p = 0.8

5.2 Head Effect

The numerical solutions of the Rayleigh-Plesset equations, Figures 12 and 23 show a maximum radii decrease with the head. It can be observed also that the maximum radii reached by the bubbles, before their collapse, are smaller than in the outlet cavitation case. In Figure 24 the maximum radius reached by the smallest active nuclei is plotted versus the head. The curve obtained in the same way as in Figure 15 follows the same $H^{-\frac{1}{2}}$ law.

Nevertheless, the weak head effect on bubble sizes is not apparent during model testing, see Figures 21 and 22.

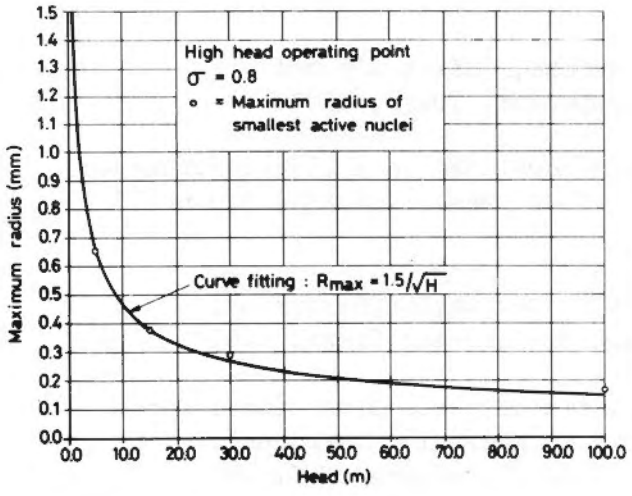

Figure 24: Maximum radius of the smallest active nuclei versus head, high head point $\sigma_p = 0.8$

6. CONCLUSIONS

The water nuclei content and the test head influence are confirmed by a numerical simulation and by experiments for travelling cavitation (separate bubbles).

The outlet cavitation behaves in a different way from the inlet cavitation in a Francis turbine.

Inlet cavitation is independent of the nuclei content and the test head.

In the outlet cavitation case, the smallest active nuclei diameter depends on the test head: it is base on an H^{-1} low (Figure 15).

Hence, only large nuclei are involved in low head tests, while the smaller nuclei are activated with higher test heads.

However, taking into account the very low nuclei content of most of the hydraulic machinery test loops (Figure 16), the nuclei injection influence plays the leading role in comparison with the head. Therefore, the nuclei content should be controlled during cavitation tests, due to its strong influence on the standard sigma measured value.

7. ACKNOWLEDGMENTS

The authors would like to thank Dominion and Vevey Engineering Works for their participation in the turbine flow calculations and Professor I.L. Ryhming and the members of the Hydraulic Machines and Fluid Mechanics Institute Cavitation Group for their valuable help.

BIBLIOGRAPHY

[1] P. Henry, Y. Lecoffre, P.Y. Larroze, "Effet d'échelle en cavitation", Proc. I.A.R.H. Symposium, Tokyo, 1980.

[2] Lord Rayleigh, "On the Pressure developed in a Liquid during the Collapse of Spherical Cavity", Phil. Mag., Vol. 34, p.94-98, August 1917.

[3] R.E.A. Arndt, "Recent Advances in Cavitation Research", Advances in Hydroscience, Vol. 12, Academic Press, 1981

[4] G. Holmes, J. McNabb, "Application of three-dimensional finite element potential flow analysis to hydraulic turbines", Proc. I.A.R.H. symposium on refined modelling of flows, Paris, September 1982.

[5] D.M. Oldenziel, "Bubble Cavitation in relation to Liquid Quality", Delft Hydraulic Laboratory Report No. 211, May 1979.

[6] R.T. Knapp, J.W. Daily, F.G. Hammit, "Cavitation", McGraw-Hill, New York, 1970

[7] J.P. Le Goff, Y. Lecoffre, "Nuclei and Cavitation", Proc. Symposium Office of Naval Research, Ann Harbor, 1982.

27.3.84